teins to exist which exhibit high selectivity and affinity towards both specific DNA sequences and different inducers.

Experimental Section

Biosensors were prepared by immobilizing the *lac* repressor protein through carbodiimide covalent coupling onto a gold surface modified with thioctic acid.[8] The *lac* repressor was purified as described previously from *Escherichia coli* BMH 8117 (genotype: F^-, Δ(*lac-pro*AB) *thi*, *gyr*A (Nal^R), *supE*, λ).[11] The Ap^R plasmid pWB1000, which constitutively overexpresses wild-type *lac* repressor, and plasmid p310, which contains the *lac* ideal operator, were cloned into the *NheI* site of plasmid pEE4.[12] Competent *E. coli* BMH 8117 cells were transformed with the plasmids according to standard procedures.[13] The cells were grown in double YT medium in 1 L culture flasks at 37 °C with shaking, harvested after 16 – 20 h of incubation, washed twice with buffer (0.2 M tris(hydroxymethyl)aminomethane – HCl (Tris-HCl; pH 7.2) containing 0.2 M KCl, 10 mM $MgCl_2$, 5 % (v/v) glycerol, 1 mM NaN_3, 0.3 mM DTT, and 1 mM phenylmethanesulfonyl fluoride (PMSF)), and stored frozen.

The plasmid DNA containing the *lac* operator was isolated from the cells harboring plasmid p310 with the miniprep Qiagen kit method according to the manufacturer's instructions. When performing measurements with linearized plasmid DNA, the plasmid DNA was digested with *Eco*RI (for the complete 2455 bp sequence) or *Eco*RI and *Hind*III (for the 84 bp sequence). The plasmids were linearized by digestion with the respective enzymes at 37 °C for 1 h.

Gold electrodes were polished, treated with ultrasound, plasma cleaned, and then pretreated with thioctic acid, as described earlier.[8] Next, the thioctic acid self-assembled electrodes were thoroughly washed with pure ethanol, dried, and activated in a 1 % solution of 1-(-3-dimethylaminopropyl)-3-ethyl-carbodiimide hydrochloride in dried acetonitrile for 5 h. After washing with 100 mM potassium phosphate buffer (pH 8), the electrodes were dipped into a protein solution (approximately 0.05 mg mL^{-1}) at 4 °C for 24 h. The electrodes were washed again with phosphate buffer and immersed for 20 minutes in a 10 mM solution of 1-dodecanethiol in ethanol. A final washing of the protein-modified electrode with phosphate buffer completed the electrode preparation.

The electrode modified with the *lac* repressor was inserted as the working electrode in a three-electrode flow cell with a dead volume of approximately 10 μL. A platinum foil and a platinum wire served as the auxiliary and reference electrodes, respectively. An extra Ag/AgCl reference electrode was placed in the outlet stream to compare the potential with the platinum reference electrode just before measurements were made. In order to apply 50 mV on the working electrode, a computer was used to compare the potential of the Pt with the potential of the Ag/AgCl before applying the pulse on the working electrode. The carrier buffer (10 mM potassium phosphate buffer, pH 7.2) containing 1 mM DTT was degassed before use and pumped at a flow rate of 0.25 mL min^{-1}. Samples of 250 μL volume were injected in the carrier flow.

Measurements were made as described earlier by applying a 50 mV potential pulse and recording the current transient.[8] The current values were collected with a frequency of 50 kHz, and the first 10 values were used for the evaluation of capacitance.

Received: February 9, 2001 [Z 16590]

[1] K. S. Mattews, J. C. Nichols, *Prog. Nucleic Acid Res. Mol. Biol.* **1998**, *58*, 127 – 164.
[2] B. Müller-Hill, *Prog. Biophys. Mol. Biol.* **1975**, *30*, 227 – 252.
[3] A. Jobe, S. Bourgeois, *J. Mol. Biol.* **1973**, *75*, 303 – 313.
[4] M. Matsuura, Y. Ohshima, T. Horiuchi, *Biochem. Biophys. Res. Commun.* **1972**, *47*, 1438 – 1443.
[5] Y. Oshima, M. Matsuura, T. Horiuchi, *Biochem. Biophys. Res. Commun.* **1972**, *47*, 1444 – 1450.
[6] M. D. Barkley, A. D. Riggs, S. Bourgeois, *Biochemistry* **1975**, *14*, 1700 – 1712.
[7] A. D. Riggs, R. F. Newby, S. Bourgeois, *J. Mol. Biol.* **1970**, *51*, 303 – 314.
[8] C. Berggren, G. Johansson, *Anal. Chem.* **1997**, *69*, 3651 – 3657.
[9] I. Bontidean, C. Berggren, G. Johansson, E. Csöregi, B. Mattiasson, J. R. Lloyd, K. Jakerman, N. L. Brown, *Anal. Chem.* **1998**, *70*, 4162 – 4169.
[10] I. Bontidean, J. R. Lloyd, J. L. Hobman, J. R. Wilson, E. Csöregi, B. Mattiasson, N. L. Brown, *J. Inorg. Biochem.* **2000**, *79*, 225 – 229.
[11] A. Kumar, I. Yu. Galaev, B. Mattiasson, *Bioseparation* **1999**, *8*, 307 – 316.
[12] A. Barker, R. Fickert, S. Oehler, *J. Mol. Biol.* **1998**, *278*, 549 – 558.
[13] J. Sambrook, E. F. Fritsch, T. Maniatis, *Molecular Cloning: A Laboratory Manual*, 2nd ed., Cold Spring Harbor Laboratory Press, Cold Spring Harbor, **1989**.

Noncovalent Assembly of [2]Rotaxane Architectures**

Christopher A. Hunter,* Caroline M. R. Low, Martin J. Packer, Sharon E. Spey, Jeremy G. Vinter, Myroslav O. Vysotsky, and Cristiano Zonta

Self-organization is an attractive approach to the construction of complex molecular architectures such as grids, cages, and topological objects.[1–3] The synthesis of catenanes and rotaxanes employs noncovalent binding interactions to template the formation of the covalently interlocked structures.[4] The key noncovalent intermediate is the [2]pseudorotaxane, where a guest molecule is threaded through the plane of a macrocycle.[5, 6] The latent topological properties of this intermediate are kinetically trapped by macrocylization to give [2]catenanes or by the introduction of bulky stopper groups to give [2]rotaxanes. Recently, there have been reports of catenane structures composed of interpenetrating self-assembled macrocycles: metal – ligand interactions have been used to construct [2]catenanes from as many as eight separate molecular components (Figure 1 a).[7, 8] To date, only covalent [2]rotaxanes have been constructed using two interlocked molecules.[4, 9] Here we describe a three-molecule approach to noncovalent [2]rotaxane architectures, where the macrocycle self-assembles around a complementary guest (Figure 1 b).

[*] Prof. C. A. Hunter, Dr. M. J. Packer, S. E. Spey, Dr. M. O. Vysotsky, C. Zonta
Centre for Chemical Biology
Krebs Institute for Biomolecular Science
Department of Chemistry
University of Sheffield
Sheffield S3 7HF (UK)
Fax: (+44) 114-273-8673
E-mail: C.Hunter@Sheffield.ac.uk
Dr. C. M. R. Low, Dr. J. G. Vinter
James Black Foundation
68 Half Moon Lane, Dulwich
London SE24 9JE (UK)

[**] We thank Dr. C. J. Craven and Dr. J. P. Waltho for the 600 MHz NMR spectra. We also thank the Royal Society/NATO & FCO Chevening (M.O.V.), the Lister Institute (C.A.H.), the EPSRC (M.J.P.), and the James Black Foundation (C.Z.) for funding.

  1433-7851/01/4014-2678 $ 17.50+.50/0

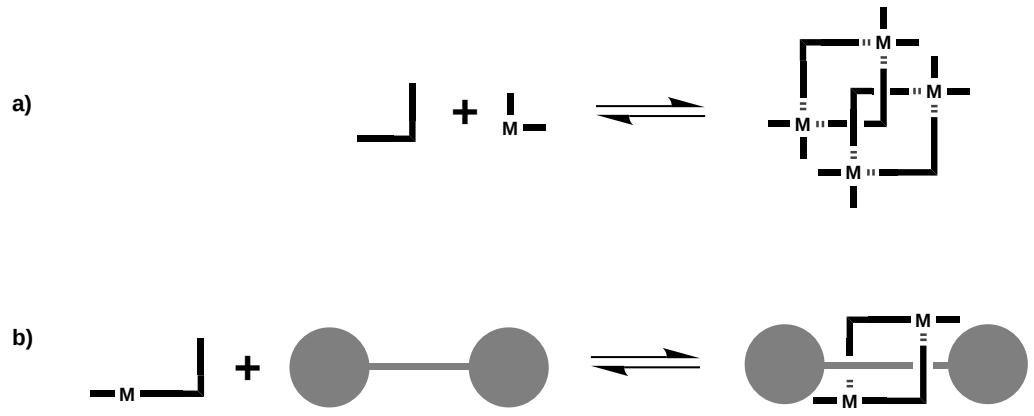

Figure 1. Self-assembly of a) [2]catenanes and b) [2]rotaxanes by using coordination chemistry.

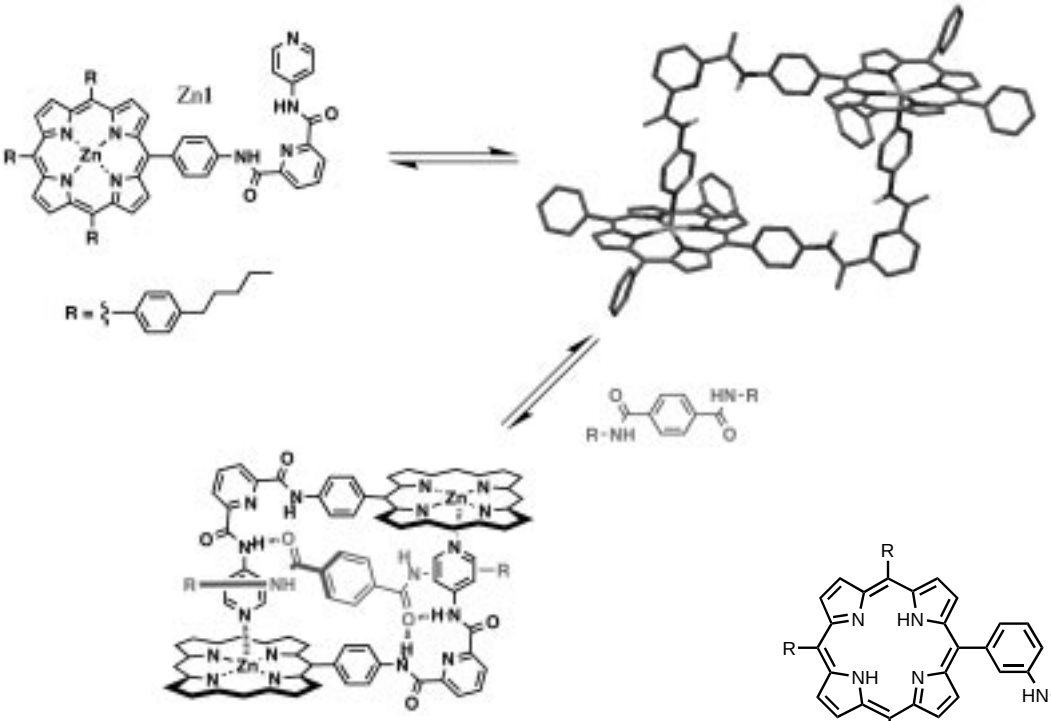

Figure 2. Zn**1** self-assembles to form a dimeric macrocyle. The X-ray crystal structure of the resulting dimer $(Zn\mathbf{1})_2$ is shown, along with a schematic diagram of the complexes formed with terephthalic acid derivatives (solubilizing groups R are omitted for clarity).

We have been studying the self-assembly of macrocyclic porphyrin oligomers through the use of coordination interactions between zinc porphyrin and pyridine.[10] Figure 2 shows the X-ray crystal structure of a macrocyclic porphyrin dimer ($(Zn\mathbf{1})_2$) that we had previously characterized by solution spectroscopy and vapor pressure osmometry and have now confirmed by crystallography.[11] Cooperativity in the macrocyclization process means that this system is exceptionally stable (the dimerization constant is $2 \times 10^8\,M^{-1}$), hence Zn**1** behaves as a macrocycle across a wide range of concentrations in noncompetitive solvents. However, the kinetic lability of the zinc–pyridine interaction means that the dimer is in dynamic equilibrium with the monomer, and here we show how this can be exploited in the construction of [2]rotaxanes.

$(Zn\mathbf{1})_2$ forms 1:1 complexes with terephthalic acid derivatives in chloroform (for diamides $K_a \approx 10^3\,M^{-1}$),[10a] and modeling studies suggest that the geometry of the complex corresponds to a pseudorotaxane architecture (Figure 2). To test this hypothesis we investigated the influence of bulky stopper groups on the dynamic properties of these complexes. Modeling studies suggested that porphyrin end-groups should be sufficiently large to function as stoppers.[12, 13] $H_4\mathbf{2}$ and a model compound **3**, which lacks the stopper groups, were therefore prepared from terephthaloyl dichloride and the corresponding amines.[14]

The ^1H NMR spectrum of mixtures of Zn**1** and $H_4\mathbf{2}$ showed signals corresponding to the pure compounds as well as a set of new resonances. Integration of these signals indicated the formation of a 2:1 complex (namely,

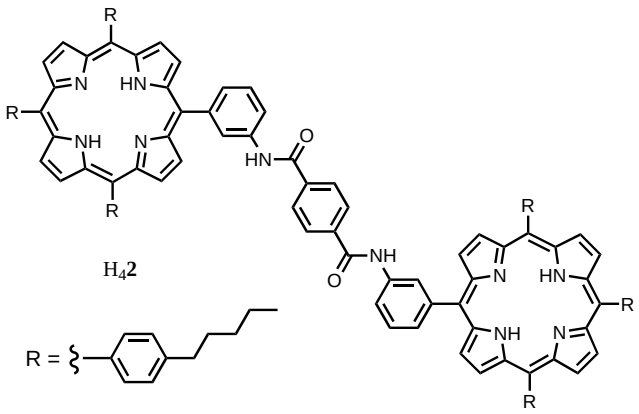

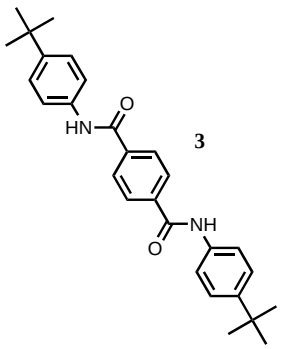

  1433-7851/01/4014-2679 $ 17.50+.50/0

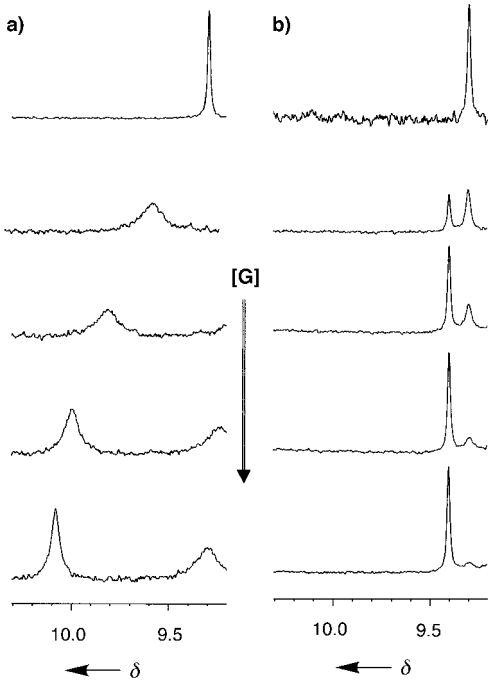

Figure 3. The amide region of the ^{1}H NMR spectra of Zn**1** (0.5 mM) in the presence of increasing amounts of guest (G; 0.2–1.2 mM). a) When the guest is **3**, the free and bound species are in fast exchange, which results in a single averaged signal (the new signal that appears at $\delta = 9.5$ towards the end of the titration is from a different amide). b) When the guest is H_4**2**, distinct slow-exchange signals are observed for the free and bound species.

$(Zn\mathbf{1})_2 \cdot H_4\mathbf{2}$) which is in slow exchange with the free species on the ^{1}H NMR timescale (Figure 3b). A titration experiment yielded an association constant of $1.8 \pm 0.4 \times 10^4\,M^{-1}$. The ^{1}H NMR spectra of mixtures of Zn**1** and **3** showed large changes in the chemical shifts of several signals relative to the corresponding spectra of the pure compounds. However, in contrast to the H_4**2** case, the free and bound species are in fast exchange in this system (Figure 3a). Titration data for the formation of the $(Zn\mathbf{1})_2 \cdot \mathbf{3}$ complex fitted to a 2:1 stoichiometry and gave an association constant of $3.3 \pm 0.9 \times 10^4\,M^{-1}$. The amide protons of $(Zn\mathbf{1})_2$ show upfield complexation-induced changes in their chemical shifts in both complexes (Figure 3), which suggests that the mode of binding for both systems is the formation of the H-bonded complex shown in Figure 2.

The ^{1}H NMR spectra of the $(Zn\mathbf{1})_2 \cdot H_4\mathbf{2}$ complex was extremely complicated, which indicates that the symmetry of both components is broken. However, COSY and ROESY spectra allowed the assignment of all the signals; the complexation-induced changes in chemical shift (CIS) relative to $(Zn\mathbf{1})_2$ and H_4**2** are shown in Figure 4a. The downfield shifts for the signals corresponding to the amide protons of $(Zn\mathbf{1})_2$ are indicative of the presence of hydrogen-bonding interactions. The upfield shift of the NH signal of the H_4**2** pyrrole group and the very large upfield shifts of the signals corresponding to the 2,6-dicarbonylpyridine groups of $(Zn\mathbf{1})_2$ suggest that there are face-to-face aromatic stacking interactions between these subunits in the complex. All of the porphyrin *meso*-phenyl groups lose their symmetry in the complex as a result of a combination of slow rotation around the porphyrin–phenyl bond and the asymmetry of the environments on the two faces of the porphyrin subunits.

Excluding the pentyl side-chains, there are a total of 59 different signals, and this system is therefore ideally suited to NMR structure determination using the CIS values.[15] In

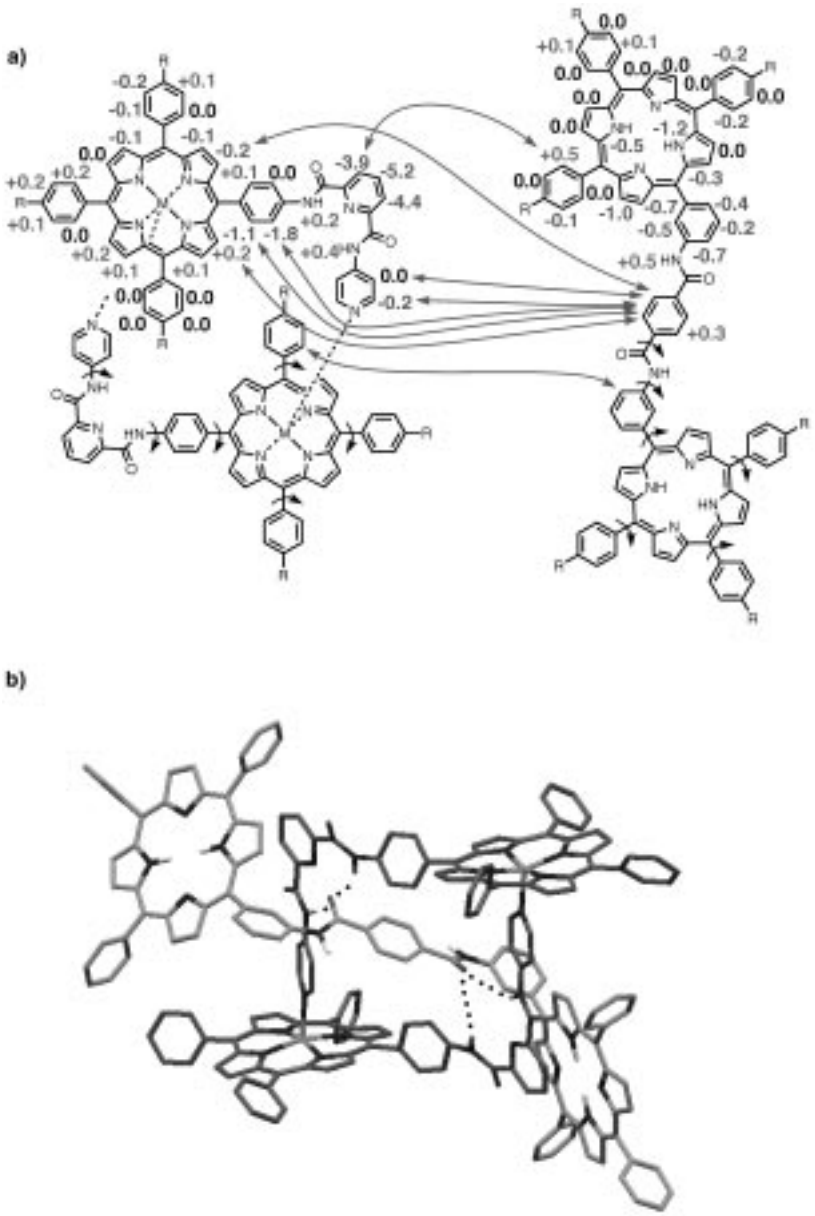

Figure 4. a) Intermolecular NOEs and CIS values obtained from the 400 MHz ROESY spectrum of $(Zn\mathbf{1})_2 \cdot H_4\mathbf{2}$ at 274 K in $CDCl_3$. The two pyrrole NH signals cannot be unambiguously assigned, but the assignment shown matches the calculated CIS values. The bonds that were allowed to rotate in the course of the conformational search are also indicated. Since both molecules have twofold symmetry, only one set of rotatable bonds is marked in each case, but all symmetry-related bonds were allowed to rotate. b) Three-dimensional structure of the $(Zn\mathbf{1})_2 \cdot H_4\mathbf{2}$ rotaxane determined from the NMR data in shown in (a).

  1433-7851/01/4014-2680 $ 17.50+.50/0 *Angew. Chem. Int. Ed.* **2001**, *40*, No. 14

addition, eight intermolecular NOEs were observed in the ROESY experiment (Figure 4a), and these are important for constraining the search space in the structure determination. The two components of the complex, $(Zn\mathbf{1})_2$ and $H_4\mathbf{2}$, were allowed to move and rotate freely relative to one another, and all of the flexible torsions (the phenyl–porphyrin and phenyl/pyridyl–amide bonds indicated in Figure 4a) were varied in the course of the conformational search. The structure for which the 59 calculated CIS values best match the experimental values is illustrated in Figure 4b (rms difference = 0.01 ppm). This structure clearly shows that the complex has the [2]rotaxane architecture illustrated in Figure 1a.

$(Zn\mathbf{1})_2 \cdot H_4\mathbf{2}$ and $(Zn\mathbf{1})_2 \cdot \mathbf{3}$ form complexes with similar structure and stability, but the kinetic properties are quite different. On heating the $(Zn\mathbf{1})_2 \cdot H_4\mathbf{2}$ complex, coalescence of some signals is observed in the ^{1}H NMR spectrum as the system moves into fast exchange, but the complexity of the spectrum and temperature-dependent changes in the populations of the free and bound species makes it difficult to reliably assign all coalescence temperatures. However, coalescence of the signals corresponding to the free and bound amide protons of $(Zn\mathbf{1})_2$ gives an activation energy of 71 ± 3 kJ mol^{-1} at 320 K.[16] On cooling the $(Zn\mathbf{1})_2 \cdot \mathbf{3}$ complex, some signals in the ^{1}H NMR spectrum broaden and split. Coalescence of the signals arising from the free and bound pyridine protons of $(Zn\mathbf{1})_2$ gives an activation energy of 60 ± 2 kJ mol^{-1} at 255 K. Thus the barrier to exchange between free and bound species is significantly larger for $(Zn\mathbf{1})_2 \cdot H_4\mathbf{2}$ than for $(Zn\mathbf{1})_2 \cdot \mathbf{3}$. We interpret this as evidence for the two different exchange pathways illustrated in Figure 5: $(Zn\mathbf{1})_2 \cdot \mathbf{3}$ forms a [2]pseudorotaxane where there is no significant barrier to exit and entry of **3** in the macrocycle, while $(Zn\mathbf{1})_2 \cdot H_4\mathbf{2}$ forms a [2]rotaxane where exit or entry of $H_4\mathbf{2}$ requires opening of the macrocycle by breaking one of the coordination bonds.

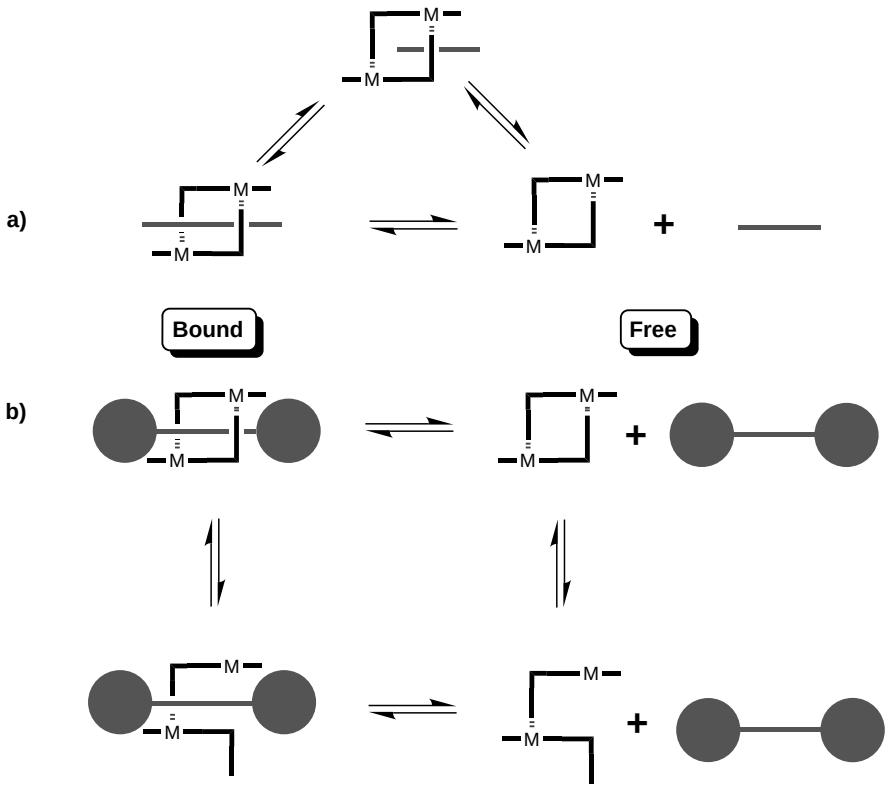

Figure 5. Pathways involved in exchange between free and bound species. a) In a pseudorotaxane, the guest slips directly out of the macrocycle. b) In a rotaxane, the macrocycle must be opened before the guest can depart.

In conclusion, we have demonstrated that self-assembled macrocycles can be used in the construction of stable [2]rotaxane architectures. The photochemical properties of the porphyrin subunits should confer this system with interesting photophysical properties: for example, singlet energy transfer between the macrocycle and axle components.[17]

Experimental Section

$H_4\mathbf{2}$: A solution of 5,10,15-tris(4-*n*-pentylphenyl)-20-(3-aminophenyl)-21*H*,23*H*-porphin[14] (0.2856 g, 0.34 mmol) and triethylamine (0.07 mL, 0.51 mmol) in dry dichloromethane (10 mL) was added to a solution of terephthaloyl dichloride (0.0172 g, 85 mmol) in dry dichloromethane (20 mL), and the reaction mixture was left stirring overnight at room temperature. After evaporation of the solvent under reduced pressure, the products were separated by column chromatography on silica gel using a mixture of dichloromethane/triethylamine (2500/1) as eluant. After recrystallization from $CHCl_3/CH_3OH$ (1/2), 0.0573 g (37%) of $H_4\mathbf{2}$ were obtained. M.p. 204–206 °C; ^{1}H NMR (400 MHz, $CDCl_3$, 20 °C, $c = 1.105 \times 10^{-3}$ M, TMS): $\delta = 8.84$ (s, 16H, CH), 8.26 (s, 2H, NH), 8.19 (d, $^3J(H,H) = 8$ Hz, 2H, CH), 8.07 (m, 12H, CH), 8.00 (br s, 4H, CH), 7.86 (s, 4H, CH), 7.68 (t, $^3J(H,H) = 8$ Hz, 2H, CH), 7.51 (m, 12H, CH), 2.91 (t, $^3J(H,H) = 7.2$ Hz, 4H, CH_2), 2.89 (t, $^3J(H,H) = 7.6$ Hz, 8H, CH_2), 1.88 (m, 12H, CH_2), 1.49 (m, 24H, CH_2), 1.01 (t, $^3J(H,H) = 7.2$ Hz, 6H, CH_3), 0.99 (t, $^3J(H,H) = 7.2$ Hz, 12H, CH_3), −2.80 (s, 4H, NH); UV/Vis (dichloromethane): λ_{max} (ε) = 648 (6900), 592 (7560), 552 (11700), 515 (20500), 419 nm (401000); FAB-MS: *m*/*z* (%): 1811 (100) $[M+H]^+$; calcd for $C_{126}H_{124}N_{10}O_2$: $[M]^+$: 1810.

3: 4-*tert*-Butylaniline (2.40 g, 16.1 mmol) was added to a solution of terephthaloyl dichloride (0.5448 g, 2.68 mmol) in dry dichloromethane (50 mL), and the reaction mixture was left at room temperature overnight with stirring. After cooling the reaction mixture to room temperature, it was evaporated to dryness under reduced pressure, then THF (50 mL) was added. The ammonium salt crystallized out of solution, and after filtration, the solution was evaporated under reduced pressure, and the white crystalline compound was recrystallized from a mixture of ethanol (63 mL) and water (13 mL). The solid was filtered and dried under vacuum for 4 h to yield 0.658 g (57%) of desired product **3**. M.p. > 270 °C; ^{1}H NMR (400 MHz, [D$_6$]DMSO, 20 °C, TMS): $\delta = 10.31$ (s, 2H, NH), 8.09 (s, 4H, CH), 7.71 (d, 4H, $^3J(H,H) = 8.9$ Hz, CH), 7.38 (d, 4H, $^3J(H,H) = 8.9$ Hz, CH), 1.29 (s, 18H, CH_3); FAB-MS: *m*/*z* (%): 429 (100) $[M+H]^+$. Elemental analysis calcd (%) for $C_{28}H_{32}N_2O_2$: C 78.47, H 7.53, N 6.53; found: C 78.63, H 7.49, N 6.42.

NMR structure determination: The method used to determine the three-dimensional structures from CIS values has been described in detail elsewhere.[15] The structure of the $(Zn\mathbf{1})_2$ dimer was taken from the X-ray crystal structure and the $H_4\mathbf{2}$ moiety was built in XED 2.8 using standard bond lengths and angles.[18] A genetic algorithm was used to optimize the conformation of the complex so that the calculated CIS values matched the experimental values as closely as possible. We allowed intermolecular

translation (±5 Å) and rotation (±180°) as well as intramolecular torsional changes (±180°) for the 24 bonds highlighted in Figure 4a. The pentyl side-chains were ignored since their conformation is not defined by the experimental data. van der Waals clashes were penalized at distances of less than 2 Å for intermolecular clashes and 1 Å for intramolecular clashes for non-hydrogen atoms. The eight NOE constraints illustrated in Figure 4a were imposed by applying a penalty if the inter-proton separation exceeded 6 Å. The search converged to a value of $R_{expt}/R_{\Delta\delta}$ of 11 in about 6000 generations for a population of 1000 (R_{expt} is the root mean square (rms) of the experimentally observed CIS values, and $R_{\Delta\delta}$ is the rms difference between the calculated and experimental values).

Received: February 12, 2001 [Z16598]

[1] J.-M. Lehn, *Supramolecular Chemistry—Concepts and Perspectives*, VCH, Weinheim, **1995**.

[2] a) N. Branda, P. Wyler, J. Rebek, Jr., *Science* **1994**, *263*, 1267–1268; b) K. D. Shimizu, J. Rebek, Jr., *Proc. Natl. Acad. Sci. USA* **1995**, *92*, 12403–12407; c) B. Olenyuk, A. Fechtenkotter, P. J. Stang, *J. Chem. Soc. Dalton Trans.* **1998**, 1707–1728; d) M. Fujita, S.-Y. Yu, T. Kusukawa, H. Funaki, K. Ogura, K. Yamaguchi, *Angew. Chem.* **1998**, *110*, 2192–2196; *Angew. Chem. Int. Ed.* **1998**, *37*, 2082–2085.

[3] a) D. B. Amabilino, J. F. Stoddart, *Chem. Rev.* **1995**, *95*, 2725–2828; b) S.-G. Roh, K.-M. Park, G.-J. Park, S. Sakamoto, K. Yamaguchi, K. Kim, *Angew. Chem.* **1999**, *111*, 672–675; *Angew. Chem. Int. Ed.* **1999**, *38*, 638–640.

[4] a) P. R. Ashton, E. J. T. Chrystal, P. T. Glink, S. Menzer, C. Schiavo, N. Spencer, J. F. Stoddart, P. A. Tasker, A. J. P. White, D. J. Williams, *Chem. Eur. J.* **1996**, *2*, 709–728; b) P. N. W. Baxter, H. Sleiman, J.-M. Lehn, K. Rissanen, *Angew. Chem.* **1997**, *109*, 1350–1352; *Angew. Chem. Int. Ed. Engl.* **1997**, *36*, 1294–1296; c) C. Gong, H. W. Gibson, *Angew. Chem.* **1998**, *110*, 323–327; *Angew. Chem. Int. Ed.* **1998**, *37*, 310–314; d) R. E. Gillard, F. M. Raymo, J. F. Stoddart, *Chem. Eur. J.* **1997**, *3*, 1933–1940; e) M. Gomez-Lopez, J. F. Stoddart, *Bull. Soc. Chim. Belg.* **1997**, *106*, 491–500; f) D. A. Leigh, A. Murphy, J. P. Smart, A. M. Z. Slawin, *Angew. Chem.* **1997**, *109*, 736–756; *Angew. Chem. Int. Ed. Engl.* **1997**, *36*, 728–732; g) S. Anderson, H. L. Anderson, *Angew. Chem.* **1996**, *108*, 2075–2078; *Angew. Chem. Int. Ed. Engl.* **1996**, *35*, 1956–1959; h) H. L. Anderson, M. R. Craig, T. D. W. Claridge, M. G. Hutchings, *Chem. Commun.* **1999**, 1537–1538; i) A. Lütringhaus, F. Cramer, H. Prinzbach, F. M. Henglein, *Justus Liebigs Ann. Chem.* **1958**, *185*, 183; j) R. S. Wylie, D. H. Macartney, *J. Am. Chem. Soc.* **1992**, *114*, 3136–3138; k) G. Wenz, E. von der Bey, L. Schmidt, *Angew. Chem.* **1992**, *104*, 758–710; *Angew. Chem. Int. Ed. Engl.* **1992**, *31*, 783–785.

[5] P. R. Ashton, D. Philp, N. Spencer, J. F. Stoddart, *J. Chem. Soc. Chem. Commun.* **1991**, 1677–1679.

[6] G. A. Breault, C. A. Hunter, P. C. Mayers, *Tetrahedron* **1999**, *55*, 5265–5293.

[7] a) M. Fujita, F. Ibukuro, H. Hagihara, K. Ogura, *Nature* **1994**, *367*, 720–723; b) M. Fujita, M. Ayoagi, F. Ibukuro, K. Ogura, K. Yamaguchi, *J. Am. Chem. Soc.* **1998**, *120*, 611; c) M. Fujita, *Acc. Chem. Res.* **1999**, *32*, 53–61.

[8] A. C. Try, M. M. Harding, D. G. Hamilton, J. K. M. Sanders, *Chem. Commun.* **1998**, 723–724.

[9] During the course of this work, a related rotaxane structure was reported in which the cyclic component was closed by coordination interactions; see K.-S. Jeong, J. S. Choi, S.-Y. Chang, H.-Y. Chang, *Angew. Chem.* **2000**, *112*, 1758–1761; *Angew. Chem. Int. Ed.* **2000**, *39*, 1692–1695.

[10] a) C. A. Hunter, L. D. Sarson, *Angew. Chem.* **1994**, *106*, 2424–2427; *Angew. Chem. Int. Ed. Engl.* **1994**, *33*, 2313–2316; b) X. Chi, A. J. Guerin, R. A. Haycock, C. A. Hunter, L. D. Sarson, *J. Chem. Soc. Chem. Commun.* **1995**, 2567–2569; X. Chi, A. J. Guerin, R. A. Haycock, C. A. Hunter, L. D. Sarson, *J. Chem. Soc. Chem. Commun.* **1995**, 2563–2565.

[11] Crystal data for $C_{142}H_{132}N_{16}O_4Zn_2$, $M_r = 2257.38$, crystallizes from chloroform as purple blocks, crystal dimensions $0.18 \times 0.16 \times 0.07$ mm. Triclinic, space group $P\bar{1}$ (C_i^1, no. 2), $a = 11.676(7)$, $b = 16.849(10)$, $c = 17.478(11)$ Å, $\alpha = 116.307(12)$, $\beta = 100.205(14)$, $\gamma = 95.904(13)°$, $U = 2969(3)$ Å^3, $Z = 1$, $\rho_{calcd} = 1.263$ Mg m^3, $Mo_{K\alpha}$ radiation ($\lambda = 0.71073$ Å), $\mu(Mo_{K\alpha}) = 0.468$ mm^{-1}, $F(000) = 1188$. Data collected were measured on a Bruker Smart CCD area detector with Oxford Cryosystems low-temperature system. Cell parameters were refined from the setting angles of 78 reflections (range $1.34 < \theta < 28.47°$). Crystallographic data (excluding structure factors) for the structure reported in this paper have been deposited with the Cambridge Crystallographic Data Centre as supplementary publication no. CCDC-157703. Copies of the data can be obtained free of charge on application to CCDC, 12 Union Road, Cambridge CB2 1EZ, UK (fax: (+44) 1223-336-033; e-mail: deposit@ccdc.cam.ac.uk

[12] P. R. Ashton, I. Baxter, M. C. T. Fyfe, F. M. Raymo, N. Spencer, J. F. Stoddart, A. J. P. White, D. J. Williams, *J. Am. Chem. Soc.* **1998**, *120*, 2297–2307.

[13] a) J.-C. Chambron, S. Chardon-Noblat, A. Harriman, V. Heitz, J.-P. Sauvage, *Pure Appl. Chem.* **1993**, *11*, 2343–2349; b) J.-C. Chambron, J.-P. Sauvage, *Chem. Eur. J.* **1998**, *4*, 1362–1366.

[14] M. Gardner, A. J. Guerin, C. A. Hunter, U. Michelsen, C. Rotger, *New J. Chem.* **1999**, 309–316.

[15] C. A. Hunter, M. J. Packer, *Chem. Eur. J.* **1999**, 5, 1891–1897.

[16] J. Sandström, *Dynamic NMR Spectroscopy*, Academic Press, London, **1982**, p. 77–123.

[17] R. A. Haycock, A. Yartsev, U. Michelsen, V. Sundstrom, C. A. Hunter, *Angew. Chem.* **2000**, *112*, 3616–3619; *Angew. Chem. Int. Ed.* **2000**, *39*, 3762–3765.

[18] J. G. Vinter, *J. Comput. Aided Mol. Des.* **1994**, *8*, 653–668.

Synthetic seco Forms of (−)-Diazonamide A**

Jing Li, Xin Chen, Anthony W. G. Burgett, and Patrick G. Harran*

Diazonamide A (**1**, Scheme 1) is a uniquely structured peptide metabolite whose potential pharmacological value and low natural abundance[1] have fueled an interest in its preparation—a pursuit that continues to gain momentum.[2] Our studies[3] in this area have centered upon a ring-contracting glycol rearrangement that stereoselectively assembles a central diazonamide C10 triarylacetaldehyde. Elaborations on this core provide intermediate **2**, wherein D/E biaryl synthesis was to occur through oxidation; the event timed late to obviate consideration of fixed axial chirality maintained in the eastern region of **1**.[2c,h] Notably, both aerobic and anaerobic oxidations of **2** generate biaryl ether **3** rather than the target D/E biaryl compound.[4] This fact was not directly recognized and experiments attempting to transform **3** into **1** would come to highlight additional limitations of the design; particularly in its provisions for oxidation state adjustment at C11 and peripheral halogenations. These

[*] Prof. P. G. Harran, J. Li, X. Chen, A. W. G. Burgett
Department of Biochemistry
University of Texas, Southwestern Medical Center at Dallas
Dallas, TX 75390-9038 (USA)
Fax: (+1) 214-648-6455
E-mail: pharra@biochem.swmed.edu

[**] We thank Prof. Michael Roth for advice and insight and Ms. Susan Jeong for invaluable experimental assistance. Funding was provided by the NIH (RO1-GM60591), the NSF (CAREER 9984282), the Howard Hughes Medical Institute (junior faculty support), and the Robert A. Welch Foundation.

  1433-7851/01/4014-2682 $ 17.50+.50/0